A Real Multitechnology Microgrid in Venice: A Design Review

A Real Multitechnology Microgrid in Venice: A Design Review

MASSIMO GUARNIERI,
ANGELO BOVO,
ANTONIO GIOVANNELLI,
and PAOLO MATTAVELLI

A microgrid currently under construction in Venice, Italy, is part of a plant for testing quasi-zero-emission processes. It has a 400-V ac bus and works islanded and connected. It includes three renewable-source generators and five energy storage (ES) systems (ESSs), based on lithium (Li), lead (Pb), sodium (Na), vanadium, and hydrogen. The hierarchical control uses a master system (Li battery) and slave systems. An energy management system (EMS) with a supervisory-control-and-data-acquisition-like architecture controls the microgrid, providing such features as anti-islanding, low-voltage ride through, and black start. The EMS performs acquisition, processing, and storage of the data produced by power network analyzers. An advanced human interface ensures flexible operation management and

performance analyses. This article presents the design of this multitechnology microgrid, which is part of an industrial pilot plant aimed at promoting a number of decarbonized technologies.

Overview of Microgrids

Electrical grids are evolving rapidly toward smart, self-regulating systems capable of managing distributed generation from intermittent renewable sources. Apart from hydroelectric, the large majority are photovoltaic (PV) systems grasping the fluctuating solar radiation and wind turbines capturing fickle wind energy, but other sources, which are at different stages of development, also generate energy with predictable or unpredictable intermittency [1]–[3].

Several investigations have highlighted that, when power production from intermittent sources exceeds 20% of the total generation, the grid may face instabilities that can evolve into blackouts [4]–[6]. ES is a measure to balance source-load mismatches and avoid such occurrences [7]–[9], but it can also provide a number of additional services that are part of the smart-grid paradigm [10]–[13]. The operation of ESSs depends on the interface converters that manage the power flow and on the supervisors who control them according to the ESS, grid, and load features [14]. Furthermore, the transmission system operator may impose constraints on the ESS operation, such as the obligation of contributing to primary regulation [15]–[17].

Several numerical analyses have been developed to investigate the behavior of electrical grids provided with energy generation from renewable sources and ES, either islanded or connected to the national/transnational grid (hereafter, just *grid*) [18]. Patsios et al. have proposed an electro-thermo-chemical model that integrates battery chemistry, power electronic, and grid for fast evaluation of the performance of a Li-ion ESS connected to a grid with distributed generation [19]. Bussar et al. provided a numerical investigation of the impact of renewable sources and storage systems in the European grid in view of the 2050 European Commission's targets performed with the free code GENESYS [20], but results appear burdened by some not completely motivated assumptions on ESSs. However, few studies have been presented on the experimental testing in real conditions of such assets installed in an islanded/connected grid.

On the household scale, Bila et al. have developed an experimental investigation of a Li-ion ESS provided with a two-quadrant converter for assessing the limitation in round-trip efficiency (RTE) and current harmonics [21]. Liu et al. presented the conceptual design and simulations of a hybrid ac/dc microgrid aimed at reducing energy conversion losses while maintaining stable operation [22]. Moreover, Hossain et al. [23] presented a review of existing microgrids projects and several other examples also available in the literature [24]. However, large experimental plants, especially with different ES technologies, on the scale of smart grids and microgrids, are rare in the scientific literature.

The MATTM Project in Venice

In view of the expansion of carbon-free systems, the Venice Municipality has planned to boost the use of renewable sources and industrial processes. In this framework, the public regional multiutility Veneziana Energia Risorse Idriche Territorio Ambiente Servizi (VERITAS) was commissioned to build an industrial test plant in Venice for the decarbonized generation, storage, and use of energy, with the financial support of the Italian Ministry for Environment and Land and Sea Protection (Ministero dell'Ambiente e della Tutela del Territorio e del Mare). The plant includes the following units (Figure 1):

1) two renewable power sources (RPSs)
2) five ESSs
3) third-generation biodiesel fuel production from exhausted oils and microalgae with emission reduction
4) bioadditive production by means of nanotechnologies, biotechnologies, and superfluids
5) supercritical chemical processes for waste treatment operating at near-zero impact
6) prototype hybrid-electric water vessels and road vehicles powered by produced biofuels.

Microgrid

The electrical part of the plant constitutes a microgrid, powered by RPSs (item one) and ESSs (item two), whereas the processes three, four, and five are the loads (Figure 2). Other key components are the grid connection controller (GCC) and the EMS, which are described hereafter together with the power units (i.e., RPSs and ESSs). The microgrid bus is powered with three-phase alternating current at 400-V root mean square (rms). RPSs and ESSs are connected to the bus via their power management systems (PMSs), which include several power electronics converters with different operating modes, as outlined hereafter.

RPSs

The two RPSs, with a total rated power of 901 kW (218 kW in islanded modes), are

- a biodiesel engine-generator (BDEG) rated 170 kW at 400 Vac that works on plant-produced fuel (Berica Impianti, Arzignano, Italy)
- a PV system (PVS) rated 731 kW (peak) at 400 Vac; it consists of a 48-kW subsystem, PVS-A, intrinsically part of the microgrid and a 683-kW subsystem, PVS-B, directly connected to the grid (Tumiati Impianti, Porto Viro, Italy).

Electrochemical ES Facilities

Different technologies for storing energy are available, some being mature and some already on the market but under further development. Others are in an early stage of research and development. Among them, electrochemical ESs (ECESs) are particularly suitable for smart grids, minigrids, and microgrids, because their inherent modularity allows a wide power and energy scalability [25], [26] that is precluded by other technologies [27]. In addition, they exhibit site versatility, near-zero environmental impact, static structure, and silent and easy operation [28], [29]. ECESs include a family of closed batteries based on different chemistries [e.g., Li,

Na, nickel (Ni), Pb], all using electrodes performing a double function: hosting the electrochemical half-reactions and also storing the converted energy.

Another ECES family consists of open devices where fluid reagents are fed in/taken from the electrodes, thus storing the converted energy outside the cells. These devices are redox flow batteries (RFBs) and hydrogen-based ESSs, consisting of an electrolyzer, a hydrogen reservoir, and a fuel cell

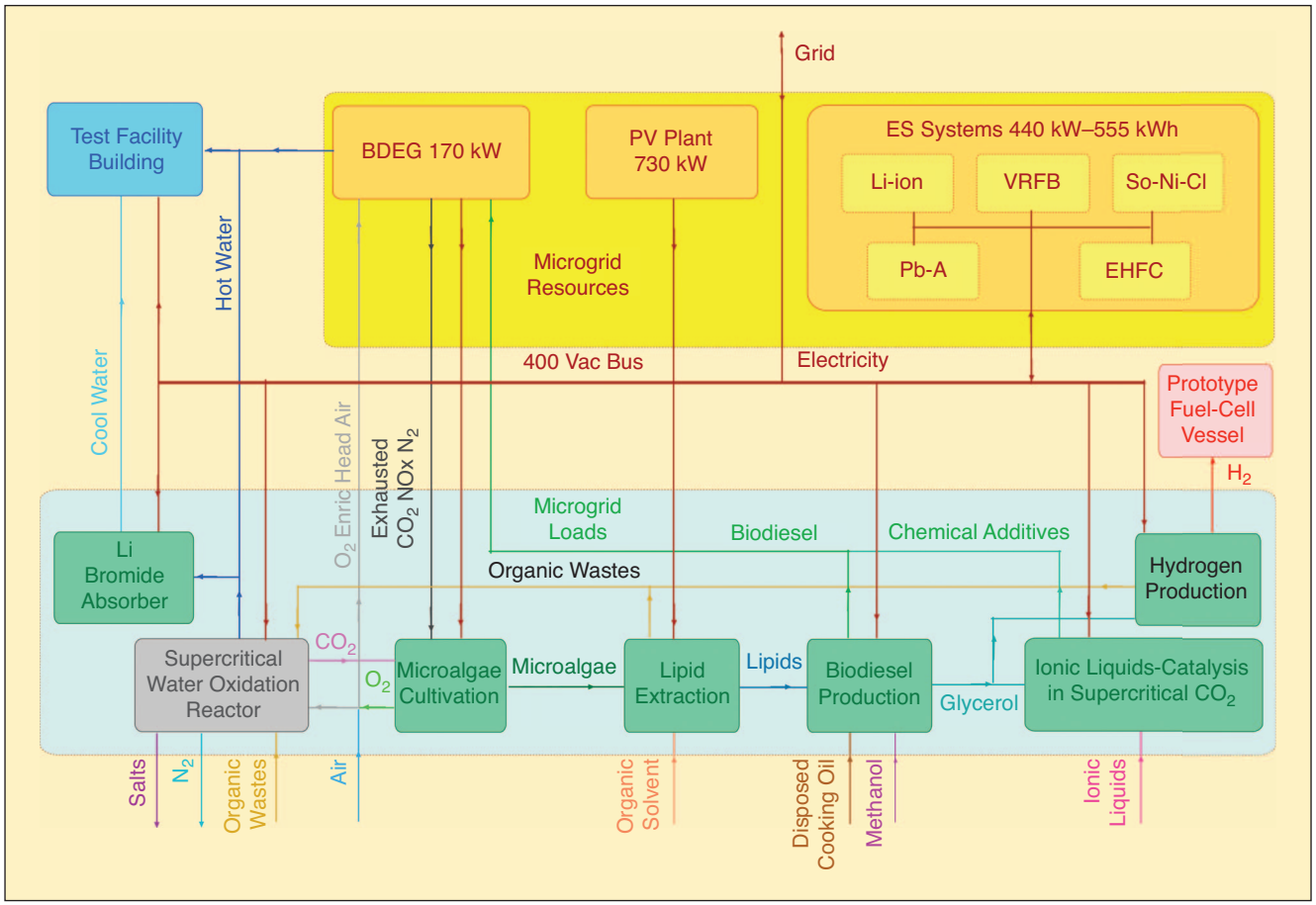

FIGURE 1 – A schematic of the industrial test plant, including the multitechnology microgrid. Colors have the following meaning: azure is the building services provided by the microgrid; orange/yellow is the microgrid resources consisting of RPSs and ECESs; green/gray is the microgrid loads consisting of carbon-free/low-emission chemical productions; and red is the hydrogen services. VRFB: vanadium RFB.

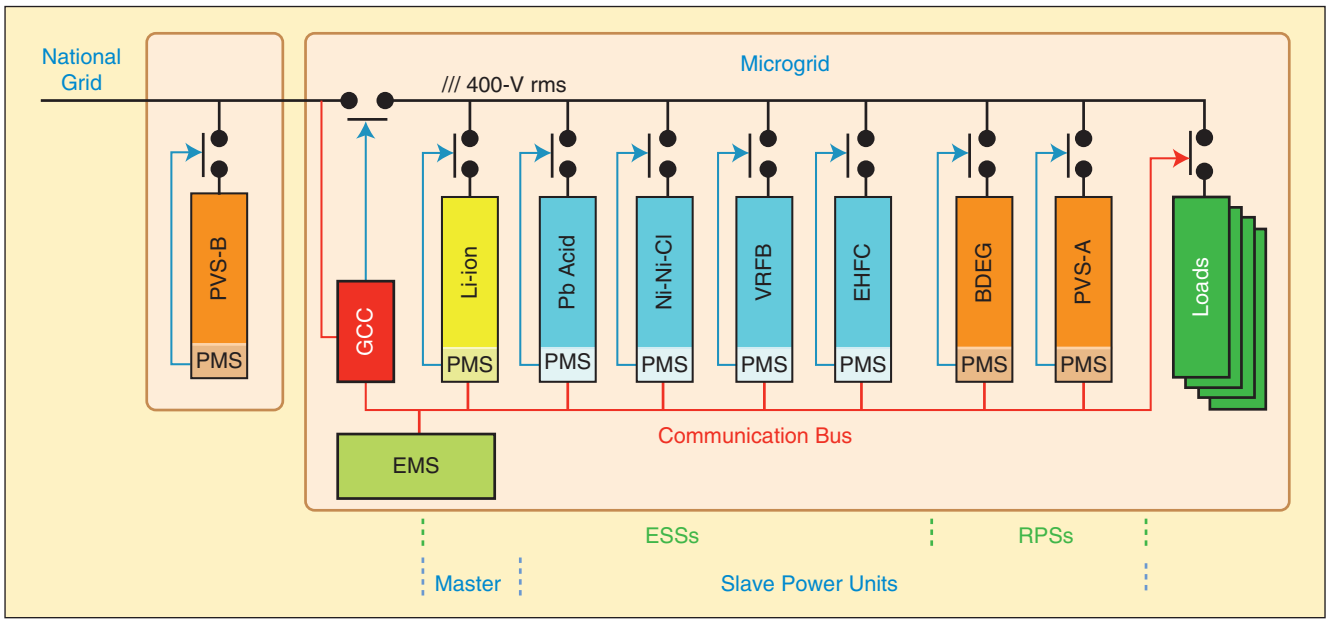

FIGURE 2 – A schematic of the microgrid, with RPSs, ESSs, GCC, and loads.

FIGURE 3 – (a) and (b) The Li-ion and Pb-acid ESS containers, both by Socomec. (Photos courtesy of Socomec.)

(EHFC). ESSs can be sized at different ranges of power, presenting different response times and discharge durations [30]. Several comparative studies on ECESs have been published, but often they do not provide complete and updated data or neglect some emerging technologies. Some authors pay little attention to RFBs, their extremely long cycle life [31], and the progress attained on their reliability in recent years, disregarding that large plants in the megawatt-megawatthour size have already been put into service worldwide, and China is installing a vanadium RFB (VRFB) station rated 200 MW–800 MWh, unparalleled by other ECESs [32]. The VERITAS microgrid is aimed at having the almost-unique feature of being provided with five different ESSs to compare their performance at the industrial level.

A number of alternative ES devices have been taken into account, considering rated power, response time, discharge duration, RTE, calendar and cycle lives, capital costs, levelized cost (i.e., lifetime costs divided by energy production), ease of maintenance, reliability, and level of technological development. Based on these criteria, the following ECES systems have been selected:

- Li-ion battery: rated 300 kW–171 kWh [0.46-h discharge duration at rated power and 80% depth of discharge (DoD), SICON-Socomec, Isola Vicentina, Italy]
- advanced Pb-acid (A-Pb-A) battery: rated 40 kW–101 kWh (2-h discharge duration at rated power and 80% DoD, SICON-Socomec, Isola Vicentina, Italy)
- Na-Ni-chlorine (Na-Ni-Cl), or zero-emission battery research activities, battery: rated 60 kW–128 kWh (1.7-h discharge duration at rated power and 80% DoD, SAET, Selvazzano Dentro, Italy)
- EHFC: rated 20 kW–5 kWh [3.5-h discharge duration at rated power and 95% DoD, Electro Power System, Paris, France; this ECES unit allows connection with the hydrogen production unit of the plant (Figure 1), based on the flexibility of hydrogen as an energy vector]
- VRFB: rated 20 kW–80 kWh (3.8-h discharge duration at rated power and 95% DoD, Gildemeister, Würzburg, Germany).

All EESs are housed in containers (Figure 3), and their total power and energy amounts to 440 kW and 556 kWh, resulting in a customized optimal sizing that does not completely conform to conventional optimum economic criteria reported in the literature [33]–[36], due to the specific experimental scope of this microgrid. Each ESS was commissioned with its own internal battery management system (BMS) and with its PMS, i.e., the dc/ac static converter for interfacing the unit with the microgrid 400-Vac bus and controlling the bidirectional power flow of the storage device.

Table 1 presents the ECES technical specifications as defined in the tendering procedure, whereas Table 2 shows the main ratings and resulting performance and cost figures obtained from the technical data of the commissioned

TABLE 1 – THE MAIN DATA OF ECES AS SPECIFIED IN THE 2015 TECHNICAL SPECIFICATION OF THE CALLS FOR BIDS.

ECES	USABLE ENERGY (kWH)	RATED POWER (kW)	DoD %	RTE %	DISCHARGE TIME (H)	CYCLE LIFE·10^3	CALENDAR LIFE (YEARS)
Na-Ni-Cl	120	60	80	60	2.5	4	1.25
VRFB	80	20	80	60	2.5	7	3.0
EHFC	20	20	80	20	0.5	0.1	1.0
Li-ion	150	300	80	70	0.3	1.5	1.25
A-Pb-A	100	40	80	60	3.5	0.8	1.0

Usable energy is a fraction of the total energy resulting from the DoD lower than 100%; discharge times are at rated powers; cycle life and calendar life correspond to a reduction to 80% of the initial capacity.

bids (costs include delivery and installation on site). Some discrepancies between the values of the two tables derive from design adjustments needed for balancing technical and economic constraints. It must be noted that, unlike the other three ECESs, the VRFB and EHFC discharge durations in Table 2 are the result of a design choice and not a limitation of the specific technology. The table also shows that Li-ion presents the highest power density, as expected, whereas the VRFB realizes the lowest levelized cost, i.e., the cost that takes into account cycle duration and RTE, thanks to the much longer cycle life. It must be noted that this is the most important cost figure according to many central administration agencies (e.g., the U.S. Department of Energy and the European Commission's Horizon 2020). In addition, thanks to the inherent decoupling between power and energy, the discharge duration of the EHFC and VRFB ESS could be extended in the future by increasing the tanks only, at a limited investment cost.

The five ESSs are designed for testing in extensive experimental campaigns under real operating conditions to compare their performance and identify the best technology for the different services required in the microgrid. Each ESS is provided with instrumentation for checking the state of health (SOH) and aging evolution. The execution of these tests is controlled by the EMS and can be run manually, automatically, or on a programmed basis. In general terms, the power converters used in the different ESSs differ both in topology and control implementation, because they are made by different producers. More specifically, the Li-ion ESS has been designed with a modular structure shaped for maximum reliability, as explained in the "Microgrid Hierarchical Structure with Master and Slave Units" section. It is made of six independent strings (Figure 4), each consisting of 12 modules rated 3.6 kWh. Each string has its own 66-kW static converter made of two 33-kW modules designed on a high-efficiency (up to 98% and 96% at low power), three-level, neutral-point clamped topology. They are provided with dynamic power control features and capability of hot module replacement, i.e., without depowering the converter [37].

Loads—Pilot Process Facilities

The microgrid loads are pilot industrial facilities operating at near-zero impact thanks to emissions reduction, thermal recovery, waste treatment, recycling, and so forth. They have an overall rated power of 140 kW (300 kVA peak) and provide the following processes: production of second- to third-generation biofuels and oleochemicals by cavitation/induction and multiphasic nanocatalysis; growth of microalgae in 3,000-L reactors for providing third-generation biofuels (biodiesel and biohydrogen), chemicals, and pharmaceuticals and reducing industrial smoke; production of biopolymers; oxidation and catalysis in reactors with supercritical environment; production of bulk chemicals (biofuels and advanced lubricants) by ionic liquids and multiphasic nanocatalysis; production of fine chemicals (intermediates and plastic polymer additives); and production of nanocatalytic hydrogen from organic alcohols.

GCC

The connection of the microgrid to the grid is performed by a motorized contactor activated by the GCC that, in turn, is controlled by the master PMS (M-PMS, described in the "M-PMS" section), under the supervision of the EMS, i.e., the supervisor of the whole microgrid. The GCC also detects the grid voltage rms values and phases as needed for proper parallel connection and provides them to the EMS. These signals are also used for proper connection of the power units (RPSs and ESSs) to the microgrid.

EMS

The EMS is the supervisor of the whole microgrid. It commands the connection of the power units (RPSs and ESSs), GCC, and loads to the microgrid bus. It also controls the PMSs of the power units, regulating their active and reactive power flows inside the microgrid and between the latter and the grid. Moreover, it activates the SOH tests of the ESSs. The EMS is described in the "EMS Architecture and Operation" section.

Electric Enclosure and Control Room

Most centralized devices and part of the peripheral units are assembled

TABLE 2 — THE MAIN DATA OF THE COMMISSIONED ECESS (2015 BIDS).

ECES	USABLE ENERGY (kWH)	RATED POWER (kW)	DoD %	RTE %	DISCHARGE TIME (H)	TEMPERATURE RANGE (°C)	CYCLE LIFE $\cdot 10^3$	CONTAINED VOLUME (M^3)	POWER DENSITY (kW/M^3)	US. EN. DENSITY (kWH/M^3)	CAPEX POWER (K€/kW)	CAPEX US. EN. (K€/kWH)	LCOE (C€/kWH/CYCLES/RTE)
Na-Ni-Cl	104	60	80	90	1.73	–30/+60	4.5	27.4	2.19	3.80	3.55	2.05	54.8
VRFB	72	20	90	63	3.60*	–23/+48	20	45	0.44	1.60	8.35	2.32	18.4
EHFC	69	20	92	24	3.45*	–20/+45	0.3	48.0	0.42	1.44	7.05	2.04	2,838.2
Li-ion	136.8	300	80	87	0.46	–20/+40	4.0	54.0**	5.56	2.53	0.71	1.56	47.5
A-Pb-A	80	40	80	75	2.00	0/+40	0.8	28.5	1.40	2.81	1.92	0.96	160.4

Discharge times refer to effective used energy at rated power; contained volumes and cost figures include ancillaries and PMSs for connecting the ECES to a 400-Vac bus. CAPEX: capital expenditure; LCOE: levelized cost of energy; US. EN.: usable energy. *VRFB and EHFC discharge durations result from design choices (are not a technological limitation, as in the other three ECESs). **Li-ion volume is affected by the topology adopted for providing redundancy, high reliability, and hot replacement.

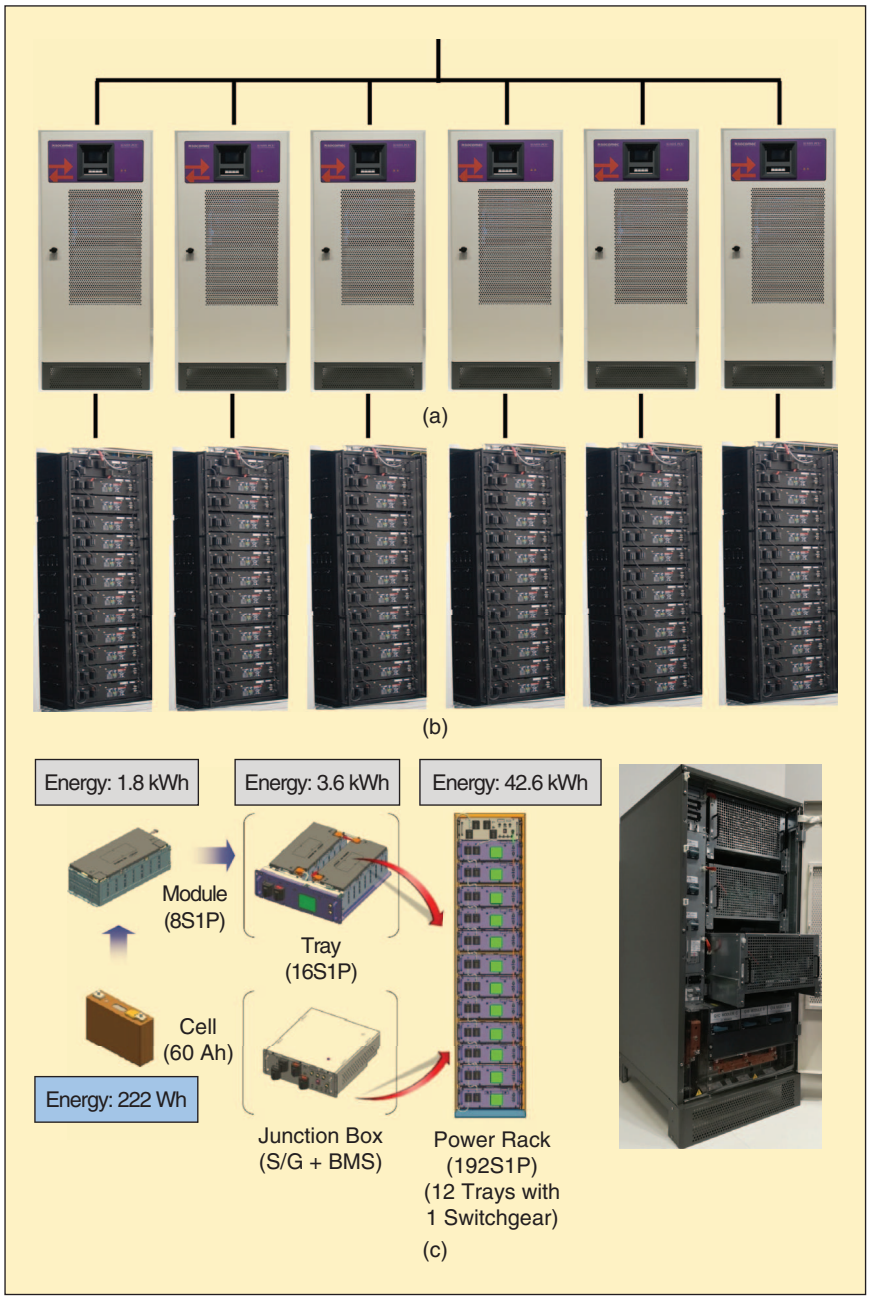

FIGURE 4 – (a) and (b) The modular architecture of the Li-ion EES (master unit), provided with hot replacement feature [evidenced in (c)].

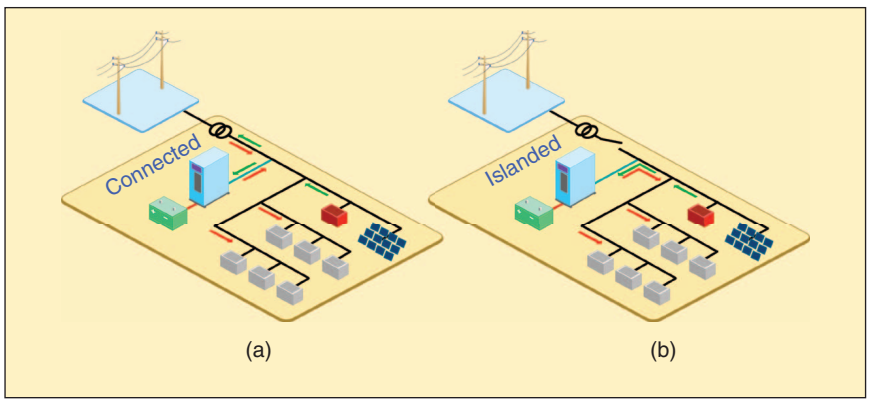

FIGURE 5 – A schematic of the microgrid operating as (a) grid-connected and (b) islanded.

into panels located in the microgrid electric enclosure, which also includes all conventional ancillaries of an electric plant. The GCC and a major part of the EMS are located in this electric enclosure. A specific room, the control room, hosts the operator and the engineer-in-charge stations, controlling and monitoring the entire plant.

Operation Modes

The microgrid can operate in three modes. In all of them, measures are enforced to provide the microgrid with resilience for fast recovery from critical conditions. The operation modes are described hereafter, together with the black start (Figure 5). A few examples of the preliminary operation of the microgrid are also reported.

- *Grid connected*: This mode occurs when the microgrid is connected to the grid. Operation complies with the CEI 0-16 standard of the Italian regulatory agency Comitato Elettrotecnico Italiano, which conforms to the Comité Européen de Normalisation Electrotechnique and International Electrotechnical Commission standard [41]. Anti-islanding measures are implemented, giving the microgrid the capability to remain connected despite minor and short grid faults [38]–[40]. Robust grid-connected operation is ensured by low-voltage-ride-through (LVRT) capability, allowing the microgrid to stay connected in case of minor voltage sags in the grid [42].
- *Intentional islanding*: This stand-alone operation occurs when the microgrid is intentionally disconnected from the grid. In this condition, the microgrid must operate at a proper level of power quality, i.e., stable frequency and voltage and reduced harmonic content [43]. The intentional opening of the GCC that trips the islanded operation must produce no disturbance in the microgrid. Protection measures are provided against accidental contacts with components still powered by the RPSs and ESSs. An example of intentional disconnection in 36-kW resistive-load condition is reported

in Figure 6(a), showing that the microgrid voltage is not perturbed. Similarly, Figure 6(b) regards the microgrid reconnection to the main grid, where the small transient in the PMS current is only due to the PMS transformer insertion.

- *Unintentional islanding*: This standalone operation occurs when the GCC automatically opens to disconnect the microgrid from the grid because of some critical condition. The automatic opening is designed to cause minimal disturbance in the microgrid, while the ESSs ensure power continuity [44]. An example of unprogrammed disconnection of the grid with negligible voltage perturbation at the microgrid side is reported in Figure 6(c).
- *Black start*: A black start consists of powering up the microgrid when disconnected to set an islanded mode, without synchronization and auxiliary power from the grid. An example of black-start operation is reported in Figure 6(d), where the microgrid voltage is formed, being still disconnected to the main grid (signal Ch4 is high). Then the grid is made available (closing the related switch), and the microgrid is connected to the main grid (signal Ch4 becomes low).

The efficient operation of a microgrid requires advanced control strategies to stabilize voltage and frequency.

Microgrid Hierarchical Structure with Master and Slave Units

The efficient operation of a microgrid requires advanced control strategies to stabilize voltage and frequency,

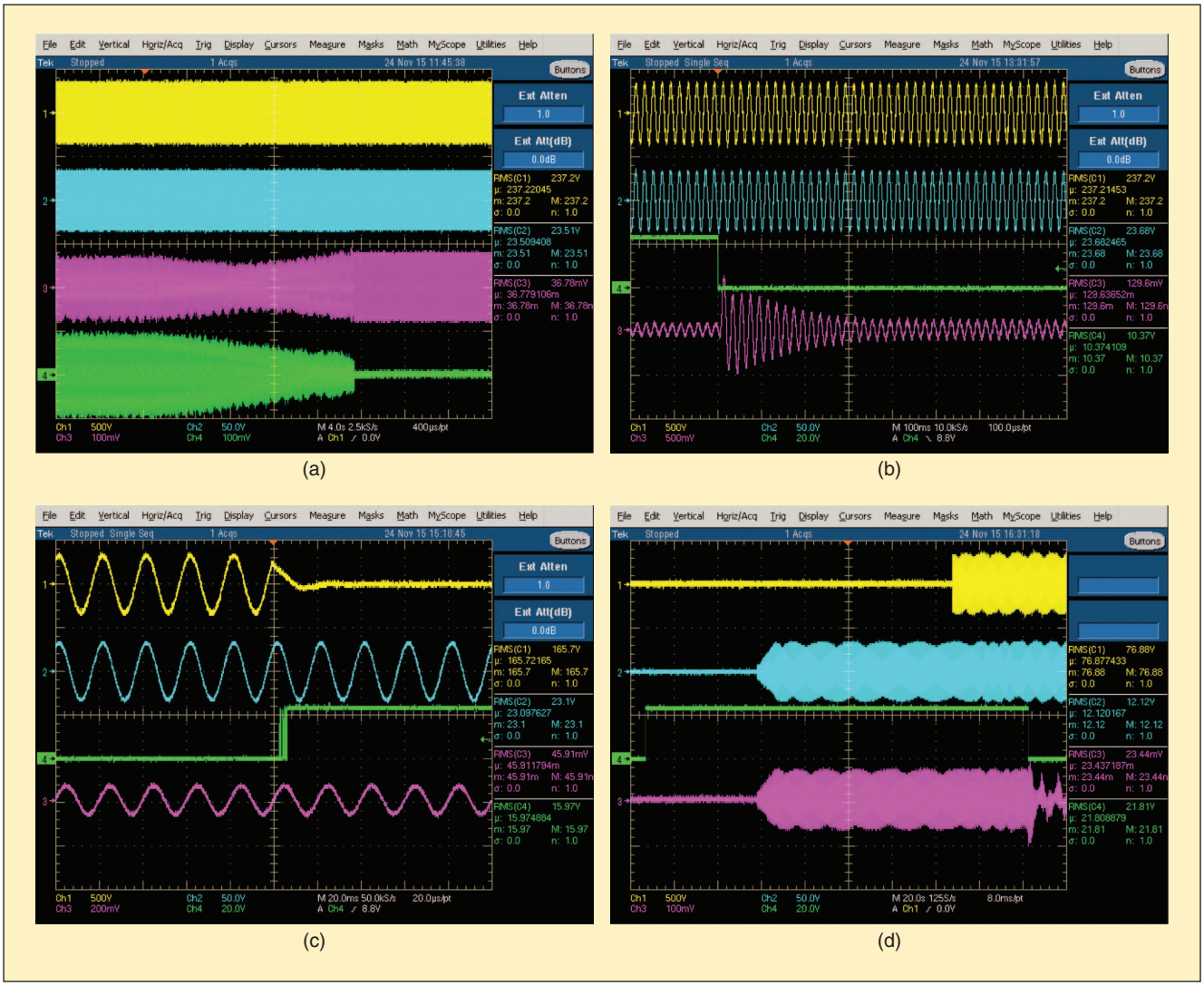

FIGURE 6 – The operation tests. (a) Intentional disconnection of the main grid. From top to bottom, CH1: Vgrid 500 V/div; CH2: Vμgrid 500 V/div; CH3: IPMS 100 A/div; CH4: Igrid 100 A/div. (b) Reconnection of the microgrid to the main grid. From top to bottom, CH1: Vgrid 500 V/div; CH2: Vμgrid 500 V/div; CH3: reclosing signal 20 V/div; CH4: IPMS 100 A/div. (c) Unprogrammed disconnection of the main grid due to GCC switch off. From top to bottom, CH1: Vgrid 500 V/div; CH2: Vμgrid 500 V/div; CH3: signal from grid disconnection switch, 20 V/div; CH4: IPMS 100 A/div. (d) Black start. From top to bottom, CH1: Vgrid 500 V/div; CH2: Vμgrid 500 V/div; CH4: signal from grid disconnection switch, 20 V/div; CH3: IPCS 100 A/div.

The control of the ESSs is a crucial aspect of the microgrid operation.

particularly in the islanded mode. Moreover, the integration in the microgrid of intermittent renewable energy sources (RESs) and ES capabilities enhances the challenge of providing reliable operation and control. Control problems are often classified into three levels, the first two pertaining to the microgrid itself and the third related to the grid [45]. The droop control and model predictive control are two example of successful control approaches used in these problems. In the present application, the droop control consists in controlling the active and reactive powers against frequency and voltage variations, in which the power set point is changed proportionally to frequency/voltage values deviations from the nominal values. Low-frequency/voltage values call for more active/reactive power, whereas high-frequency/voltage values call for less active/reactive power. The droop control is performed locally by each unit that is capable of active power control (e.g., ESSs, biodiesel generator). The predictive control uses forecast data (based on regression models for loads and weather forecasts affecting PV production) to predict the overall system energy balance and choose which control strategy provides the best fit with the predicted scenario.

A hierarchical control structure organized in three levels suitable for different control approaches and capable of efficient stationary and dynamic performance has been presented by Bidram and Davoudi [46]. In the present application, the three-level control, aimed at enabling augmented control effects, operates as follows.

1) The first level is implemented in each unit, and its programmable logic performs simple actions to preserve the microgrid stability, such as droop control or managed system shutdowns when no connection is available with the central control system (second level).
2) The second level is implemented in the EMS and provides centralized commands to the units based on a holistic approach, because it knows everything about the microgrid. This level implements real-time data-based optimizations, according to design specifications, and corrects level-one errors of the droop control by changing droop parameters.
3) The third level is still implemented on the EMS and decides which control strategies have to be selected on the second control level based on midterm data forecast, while providing long-term data logging for the operator and high-level interface.

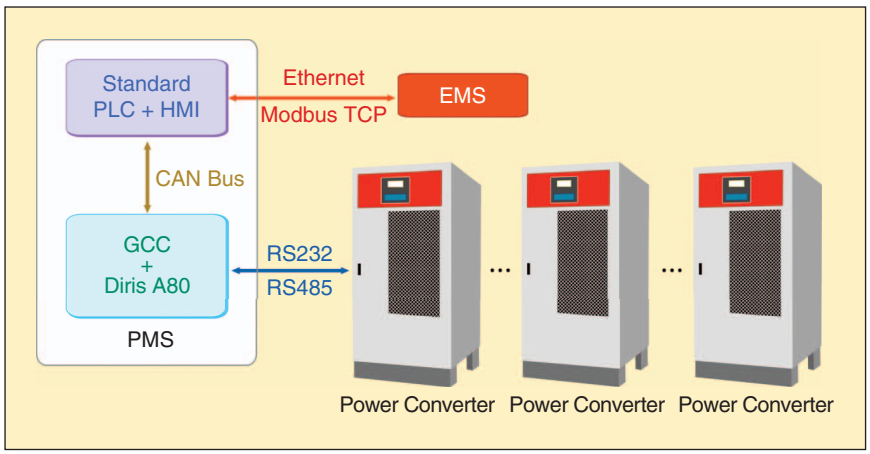

FIGURE 7 – The architecture of the master PMS, controlling the power flow through power converters of the Li-ion EES. CAN: controller area network.

A proper operation strategy consists of minimizing all microgrid losses and power flow for voltage regulation. The globally optimal solution of this nonconvex problem can be found by resorting to some optimization technique. The procedure proposed by Dall'Anese et al. that makes use of semidefinite programming [47] is one possible solution. In a microgrid containing several independent systems, any of them must provide its phase and voltage control as required by mutual synchronization and by grid-connected operation. Our microgrid has been designed with a single central control and with one unit operated as master, consisting of the Li-ion battery ESS, which is controlled as a voltage source. All other power units (ESSs and RPSs) are operated as slave generators controlled as current sources. This architecture allows for simplifying unit synchronization and the microgrid connection to the grid. The modular architecture of the Li-ion ESS, described previously, assures a high level of reliability and fault resiliency. In the unlikely event that it fails anyway, the BDEG takes over as the master generator, thus ensuring additional microgrid robustness.

M-PMS

The control of the ESSs is a crucial aspect of the microgrid operation, and advanced physics-based models of the ESSs offer much more robust operation of the storage systems [48]. In our microgrid, the BMSs that provide such functions have been included in the batteries by the producers. Instead, the PMSs are designed to provide interface of the batteries with the microgrid. The M-PMS, placed inside the master unit, consists of a programmable logic controller (PLC), instrumentation, and a control board (Figure 7). The M-PMS operates as a voltage source controlled by the EMS to obtain the required active and reactive power flow from the master ESS and send back its operating parameters. The master unit operates in compliance with the CEI 0-16 standard, particularly regarding two-threshold operation in the case of LVRT.

Slave PMS

The slave PMSs (S-PMSs) of the four slave ESSs and of the two RPSs are included in the unit control circuits. When the M-PMS needs a change in the operating parameters of the slave units, it sends a request to the EMS, which forwards consistent commands to the S-PMSs. Each PMS enables the connection to the microgrid and operates its power unit as a current source for delivering the required power and sends back its operating parameters. Any slave power unit can temporarily disconnect from the microgrid in case it cannot conform anti-islanding functions and/or it cannot accept wider LVRT thresholds. The slave units operate in compliance with the CEI 0-16 standard, particularly as regards two-threshold operation in the case of LVRT.

EMS Architecture and Operation

The EMS is the microgrid's distributed supervisor, controlling the operation of the units. In particular, it commands the connection of the power units and loads to the microgrid bus and the connection of the microgrid to the grid. It also orders the PMSs to regulate their active and reactive power flows between the power units and of the microgrid and between the latter and the grid, so as to improve the power quality and minimize the overall active and reactive power demands and their inherent costs. In addition, the EMS supervises the ESS SOH tests, either manual, programmed, or automatic.

The EMS is built on a hardware–software architecture as a processing and controlling logic device capable of executing physical operations based on implemented procedures. The hardware is located in the control room, in the central low-voltage panel (CLVP) (located in the electrical enclosure) and in the 16 peripheral local low-voltage panels (LLVPs) (located in the units), as shown in Figure 8.

The EMS is designed around a three-level architecture conforming to the hierarchical structure previously described. Level one is the lower level built in the PLCs of the power units and provides real-time interfacing among the units (RPSs, ESSs, loads, and so forth), signal detection, and fast microgrid stability assurance. Level two consists of the CLVP–LLVP network and provides real-time software microgrid control in both manual and automatic operation in the short, mean, and long term. Level three is the highest level and regards monitoring and control of the units, either for generation, storage, or load, while providing human interface. It is built in a personal computer (PC) (master PC in the control room) with myLEAF software (see the "LEAF Software" section). Level-three operations can be manual or automatic and are accessible to the operator either on site or remotely via a web connection. The EMS is designed

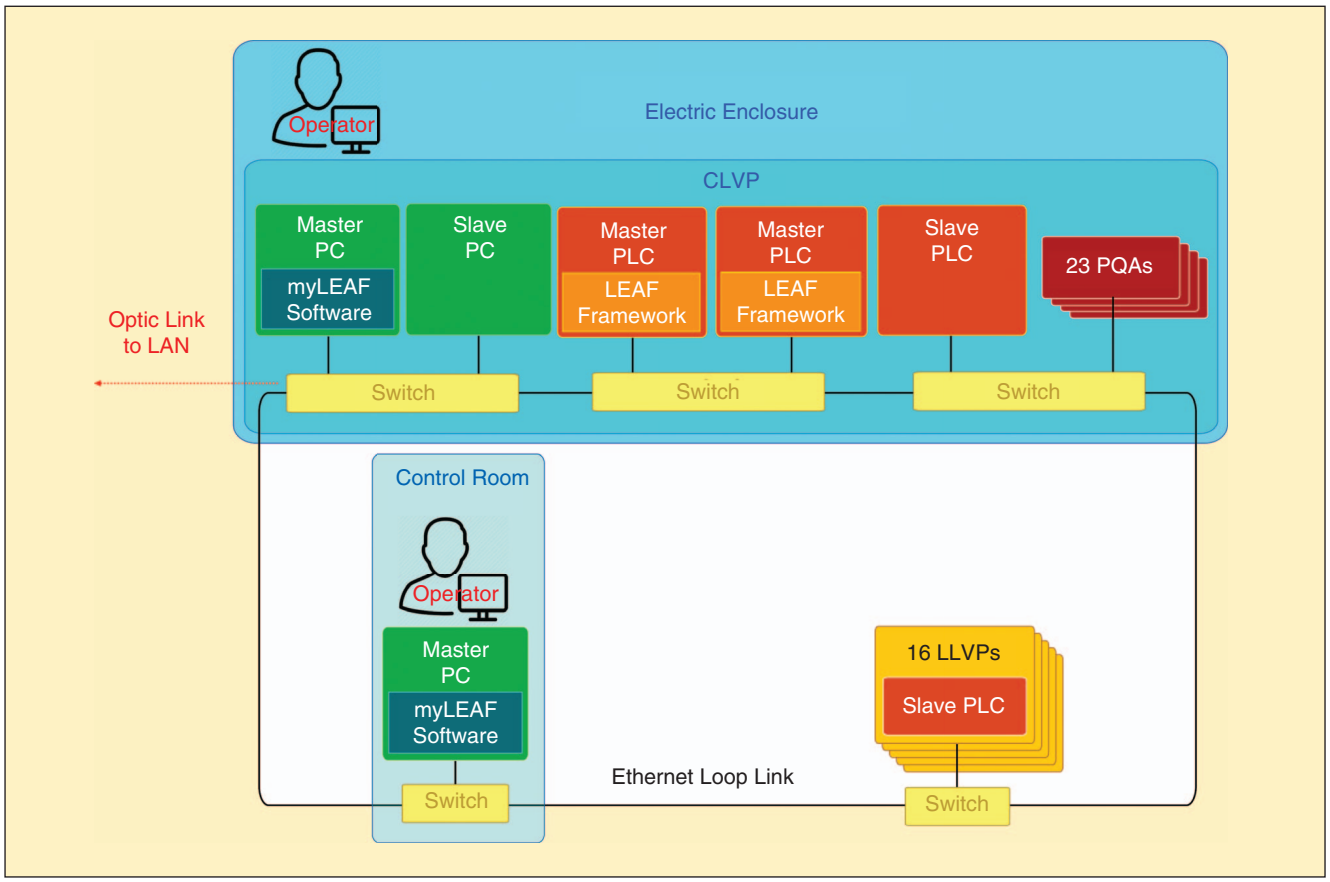

FIGURE 8 – The architecture of the EMS that controls and monitors the entire microgrid operation. The electric enclosure (upper half) includes a fully operative control position (operator) and the whole CLVP, where the two PCs (a master with partial control capacity and a slave), three PLCs (two masters and one slave), and 23 PQAs are assembled. All microgrid control functions are available at a master PC located in the control room. The 16 peripheral controlled units are interfaced via LLVPs that use slave PLCs. One-to-one interconnection among devices is provided by four switches and uses the extensible authentication protocol, whereas Modbus TCP is used between PMSs and their slave PLC. LAN: local area network.

The myLEAF software is a flexible and customizable modular platform that provides services in the energy sector.

with advanced ergonomic human–machine interface (HMI) features to facilitate comfortable operator working conditions and complies with all pertinent technical and legal regulations, notably the CEI 0-16 standard.

CLVP

The main components of the CLVP, placed in the electric enclosure, are two PCs (a master and a slave), three PLCs (two masters and a slave), and 23 power quality analyzers (PQAs). The master PC is provided with some duplicated control functions with respect to the master PC in the control room, for the sake of convenience, whereas the slave PC is a redundant device that receives the 400-Vac bus voltage parameters and supersedes in case of a fault of the master PC. Each PC is provided with four i7-4770S Intel core central processing units with a 3.9-GHz clock, 8-MB cache, 16-GB random access memory, 2-TB hard disk for data mirroring, and 22-inch touch-screen monitor. The PLCs feature a 64-b, 1,500-MHz processor and 10-MB memory with a processing speed of 1 b every 4 ns. The slave PLC controls the connection of the loads, whereas the two master PLCs (each a backup of the other for redundancy) provide the following functions:

- receive data processed by the PQAs and forward these to the higher control level of the EMS
- receive commands from the higher control level of the EMS and forward them (e.g., set-point change, unity disconnection) to the slave PLCs of the LLVPs
- detect warnings, alarms, and error signals from the units and send them to the EMS higher control level
- receive data (state of charge, ready to connect, and so on) of the ESSs for analyzing and comparing performance and actuating the control strategy.

The PQAs are high-precision analyzers that, combined with adequate current transformers, ensure accuracy classes 0.2S and 0.1. In addition, the fast response of these devices allows capturing fast events, whereas slow events are monitored and processed by the PC software. The seven PQAs interfaced with the PMSs of ESSs and RPSs consist of quality analyzer QNA 500 by ASITA (Faenza, Italy). This modular device can detect the main electrical parameters and transient disturbances, including energy flow, power consumption curves, flickers, and total harmonic distortion, with an accuracy of 0.1% for voltage and current; 0.2% for power, energy, and power factor; and 0.01 Hz for frequency. Up to 50 harmonics are analyzed. The internal memory consists of a removable 4-GB microsecure digital that makes data remotely available. The sampling rate is 512 samples per cycle, recording rate is two samples per cycle, and digitalized data are transmitted to an external memory. A remote touch-screen display features vector graphic analyzer and other synthetic indications.

The auxiliary and privileged lines of the ESSs, BDEG, and loads are also monitored but at a lower level of detail, so that the simpler model DGM 900 by Lovato Electric (Gorle, Italy) has been chosen for these functions. It is able to detect all relevant quantities (three-phase voltages and currents at 0.2%, power and energy at 0.5%, and so on) with very good accuracy. The sampling rate is 128 samples per cycle, and the recording rate is one sample per cycle. It can record up to 100 customizable events and is provided with 8-MB recording memory, touch-screen display, and data-logger features, and it conforms to the EN 50160 standard.

LEAF Software

The LEAF commercial software (Angeli di Rosora, Italy) is a package that manages and monitors in real time the microgrid and unit operations, including data logging of the electrical and physical measurements and of the microgrid status. It consists of the LEAF Framework and myLEAF packages. The LEAF Framework is a package for monitoring and controlling a system of units distributed within a microgrid for energy generation, consumption, or storage. Installed in the two master PLCs for redundancy, it constitutes the real-time control of the VERITAS microgrid. In fact, the LEAF Framework exploits the hard real-time PLC control and input/output (I/O) control to ensure the microgrid stability. It consists of a number of modules performing specific functions. The module managers, e.g., are drivers of the interfaces with the field/plant, which manage signal acquisition and command delivery according to supported protocols (controller area network, Modbus, IEC61850, and so forth).

The myLEAF software is a flexible and customizable modular platform that provides services in the energy sector. It is installed in the two master PCs and allows analysis and visualization of historical and real-time data as well as accessing data remotely within the VERITAS network via a web browser. It provides HMI in local (Windows) and web (hypertext markup language 5) environments and can be implemented with synoptic features and mobile-friendly web interfaces. Examples of these interfaces are shown in Figure 9. These tools allow flexible management and easy customization of EMS operations and also provide background services regarding logging, validation, reconstruction, and data forecasting. Some functions provided by myLEAF are displaying microgrid summary information in fully customizable dashboards, analyzing trends for each meter and historicized quantity, and scheduling and executing data validation.

LLVPs

The 16 peripheral LLVPs, which are located in the PMSs of the units, mainly consist of slave PLCs providing the unit interfaces. Specifically, they receive

the commands generated by the master PLCs and forward them to their units (as digital, analog, and RS-485); forward warnings and malfunction signals to the master PLCs; interface local I/O (digital, analog, and RS-485); provide a droop-like control of the generators that ensures network stability by means of a distributed strategy [49], [50]; and activate the connections of the loads to the microgrid (power units are controlled by their PMS instead). The detection of the microgrid voltage and frequency is provided by a local high-speed fieldbus module, whereas an integrated UPS ensures LLVP operation in the case of microgrid blackout.

Interconnection

Master and slave PLCs communicate one to one through an authentication protocol (Extensible Authentication Protocol, with 2-ms data exchange, even though other protocols are available in the communication devices) running in real-time Ethernet, which allows precise timing of information exchange, thus allowing a reliable transmission of critical data. The communication between the slave PLCs and the PMSs uses the Modbus Transmission Control Protocol (TCP), thus taking place in strictly controlled times. The distributed control network includes several nodes distributed in the microgrid: the control room, with the operator and engineer-in-charge stations; the electric enclosure with the CLVP and the LLVP of the PV-A unit; and the ESSs, RPSs, PVs, and loads, summing up to 16 LLVPs with their slave PLCs.

EMS Tasks

The EMS is designed to acquire, process, and store a number of signals to carry out every desired scientific analysis on the microgrid performance. These signals include unit and microgrid powers, voltages, and currents; ESS energies, powers, and systems-on-a-chip; grid frequency (ac side); power factor at the microgrid port; unit temperatures; rotating machine speed; fluid pressures and flows (hydrogen and redox solutions); fluid levels, volumes, and pH; device commands; and operating status. Digital analyzers perform continuous data sampling at 256 samples/cycle in normal operation and at a rate of 20 μs on the ac side in case of transient events. Data recording is performed at a rate of one sample per minute during standard operation, five samples per second during test operations, and not less than 50 samples per second during transients.

In addition, the EMS can perform the following tasks:

1) detecting the grid and microgrid (RPSs, ESSs, loads, and so on) status
2) commanding the GCC disconnection to start an intentional and unintentional islanded operation
3) setting the PMS controls based on the grid voltage parameters to control the smooth connection to the grid when switching into grid-connected mode
4) commanding the black start of the microgrid in an islanded operation
5) monitoring and controlling all PMSs
6) controlling the power flow sharing among RPSs and ESSs, according to power demands from users and ESS states of charge
7) automatically controlling the S-PMS operations based on signals from

FIGURE 9 – Screenshots showing the HMI functions of the myLEAF software: (a) controller web page, (b) device web page, (c) myLEAF's dashboard, and (d) data set web page.

the M-PMS or allowing the operator to manually control them

8) defining the medium-term strategy according to forecasts of weather, load demand, and energy price (defined by MGP, the day-ahead market of Gestore Mercati Energetici, the Italian authority for power exchange), and predefined targets or operator-defined parameters
9) commanding the EES SOH tests and analyzing their results
10) receiving and processing ESS status signals from the PMS to control its operation
11) setting the short-term energy strategy based on ESS status
12) activating the medium- to short-term strategies by sending ESS charge and discharge commands and PMS power settings, enforcing frequency regulation and stability of the microgrid when islanded
13) sending commands to the PMSs for controlling the overall and individual active and reactive power flows.

Final Remarks

This article presented the design of a real microgrid that includes three RPSs (a double PV plant and a BDEG) and five ES devices (Li-ion, Pb-A, Na-Ni-Cl batteries, EHFC, and VRFB). The microgrid is currently under construction at Venice, Italy, in the framework of national and municipal policies for promoting carbon-free energy. The microgrid design has been developed by the VERITAS company with the support of researchers from the University of Padua, Italy, and has been conceived in the logic of integration of state-of-the-art industrial technologies provided by different producers.

Tight technical specifications have been imposed to assure proper operation of the different units within the microgrid system. The producer who won the contracts demonstrated the ability to fulfill such specifications as proved in the tests performed on built units. The microgrid structure will allow comparison on a real industrial scale of different RES and ESS technologies and their collaborative operation to provide a wider knowledge on their suitability and competitiveness to the different services required by smart-grid operations, thus assessing their readiness for full exploitation. In this way, it will constitute a benchmark for future implementation of carbon-free technologies that the Venice Municipality is strongly willing to enforce, with the aim of preserving the unique heritage of the city and its lagoon.

Acknowledgments

This work was supported by the Italian Ministry for Environment and Land and Sea Protection (Ministero dell'Ambiente e della Tutela del Territorio e del Mare) under grant 17702 of the Municipality of Venice. We are grateful to the companies Loccioni and SICON-Socomec for their active contribution in the development of this project and in providing some of the material used in writing this article.

Biographies

Massimo Guarnieri (massimo.guarnieri@unipd.it) received his M.S. degree (honors) in electrical engineering from the University of Padua, Italy, in 1979 and his Ph.D. degree in electrical science in Rome directly from the Italian Ministry of Education and University in 1987. He has been a full professor at the University of Padua since 2000. He worked on the design of devices for thermonuclear fusion research for 20 years. For the last 15 years, he studied energy storage devices. He is also involved in the history of technology. He has authored more than 200 papers (130 indexed in Scopus) and books. He holds three patents. He represents the University of Padua in the European Energy Research Alliance. He is a member of the Illuminating Energy Society as well as a columnist for and member of the editorial board of *IEEE Industrial Electronics Magazine*. He is a Member of the IEEE.

Angelo Bovo (a.bovo@gruppoveritas.it) received his degree in surveying from the Giovanni Boaga Institute of Cadoneghe, Italy, in 1983 and his degree in electronic engineering from the University of Padua, Italy, in 1990. From 1990 to 1993, he was employed by Magrini Galileo Mechanics on the design of cranes. He has worked for Veneziana Energia Risorse Idriche Territorio Ambiente Servizi (VERITAS) since 1993. He worked on design of special equipment for waste collection in the historic center of Venice. He acted as responsible officer for the rational use of energy for VERITAS from 2001 to 2012 and Ecoprogetto Venezia from 2010 to 2013. Currently, his work involves designing photovoltaic and three-generation plants with biomass and gas and with designing energy storage systems from renewable sources and innovative technologies for electric mobility in the Venetian lagoon.

Antonio Giovannelli (a.giovannelli@loccioni.com) received his undergraduate degree in 2006 and his M.S. degree in 2008, both in computer science and engineering at the University of Bologna, Italy. He worked as a consultant for utility companies, developing billing procedures and metering data-management systems mainly for the free electric market. In 2011, he joined the Loccioni Group as a manager of the research and development group and head of the engineering team of the energy business unit. Since 2016, he has been a manager of the energy business unit responsible for the development of utilities' and industrial customers' services related to energy and power quality solutions and microgrid development.

Paolo Mattavelli (paolo.mattavelli@unipd.it) received his M.S. and Ph.D. degrees in electrical engineering from the University of Padua, Italy, in 1992 and 1995, respectively. Since 1995, he held faculty positions at the universities of Padua and Udine, Italy, and at the Center for Power Electronics Systems, Virginia Tech, Blacksburg. He is currently a professor with the University of Padua, leading the power electronics laboratory in Vicenza. His major fields of interest include analysis, modeling, and control of power converters; grid-connected converters for renewable energy systems and smart grids; and high-temperature and high-power density power electronics. In these fields, he has been leading several industrial and government projects. He is a Fellow of the IEEE.

References

[1] M. Liserre, T. Sauter, and J. Y. Hung, "Future energy systems: Integrating renewable energy sources into the smart power grid through industrial electronics," *IEEE Ind. Electron. Mag.*, vol. 4, no. 1, pp. 18–37, 2010.

[2] E. J. Coster, J. M. A. Myrzik, B. Kruimer, and W. L. Kling, "Integration issues of distributed generation in distribution grids," *Proc. IEEE*, vol. 99, no. 1, pp. 28–39, 2011.

[3] T. Ackermann, G. Andersson, and L. Söder, "Distributed generation: A definition," *Electr. Power Syst. Res.*, vol. 57, no. 3, pp. 195–204, 2001.

[4] T. L. Vu and K. Turitsyn, "Robust transient stability assessment of renewable power grids," in *Proc. 2016 IEEE Int. Conf. Sustainable Energy Technologies (ICSET)*, pp. 7–12.

[5] L. Hirth, "The market value of variable renewables: The effect of solar wind power variability on their relative price," *Energy Econ.*, vol. 38, pp. 218–236, July 2013.

[6] B. K. Sovacool, "The intermittency of wind, solar, and renewable electricity generators: Technical barrier or rhetorical excuse?" *Util. Policy*, vol. 17, nos. 3–4, pp. 288–296, 2009.

[7] Y. Xu, W. Zhang, G. Hug, S. Kar, and Z. Li, "Cooperative control of distributed energy storage systems in a microgrid," *IEEE Trans. Smart Grid*, vol. 6, no. 1, pp. 238–248, 2015.

[8] M. Beaudin, H. Zareipour, A. Schellenberglabe, and W. Rosehart, "Energy storage for mitigating the variability of renewable electricity sources: An updated review," *Energy Sustain. Develop.*, vol. 14, no. 4, pp. 302–314, 2010.

[9] A. Evans, V. Strezov, and T. J. Evans, "Assessment of utility energy storage options for increased renewable energy penetration," *Renew. Sustain. Energy Rev.*, vol. 16, no. 6, pp. 4141–4147, 2012.

[10] H. Chen, T. N. Cong, W. Yang, C. Tan, Y. Li, and Y. Ding, "Progress in electrical energy storage system: A critical review," *Prog. Nat. Sci.*, vol. 19, no. 3, pp. 291–312, 2009.

[11] X. Luo, J. Wang, M. Dooner, and J. Clarke, "Overview of current development in electrical energy storage technologies and the application potential in power system operation," *Appl. Energy*, vol. 137, pp. 511–536, Jan. 2015.

[12] N. Günter and A. Marinopoulos, "Energy storage for grid services and applications: Classification, market review, metrics, and methodology for evaluation of deployment cases," *J. Energy Storage*, vol. 8, pp. 226–234, Nov. 2016.

[13] J. Cho and A. N. Kleit, "Energy storage systems in energy and ancillary markets: A backwards induction approach," *Appl. Energy*, vol. 147, pp. 176–183, June 2015.

[14] J. M. Carrasco, L. G. Franquelo, J. T. Bialasiewicz, E. Galván, R. C. Portillo Guisado, M. A. M. Prats, J. I. León, and N. Moreno-Alfonso, "Power-electronic systems for the grid integration of renewable energy sources: A survey," *IEEE Trans. Ind. Electron*, vol. 53, no. 4, pp. 1002–1016, 2006.

[15] M. Müller, L. Viernstein, C. N. Truong, A. Eiting, H. C. Hesse, R. Witzmann, and A. Jossen, "Evaluation of grid-level adaptability for stationary battery energy storage system applications in Europe," *J. Energy Storage*, vol. 9, pp. 1–11, Feb. 2017.

[16] R. Hollinger, L. M. Diazgranados, F. Braam, T. Erge, G. Bopp, and B. Engel, "Distributed solar battery systems providing primary control reserve," *IET Renew. Power Gen.*, vol. 10, no. 1, pp. 63–70, 2016.

[17] F. D. Galiana, F. Bouffard, J. M. Arroyo, and J. F. Restrepo, "Scheduling and pricing of coupled energy and primary, secondary, and tertiary reserves," *Proc. IEEE*, vol. 93, no. 11, pp. 1970–1983, 2005.

[18] K. Mets, M. Strobbe, T. Verschueren, T. Roelens, F. De Turck, and C. Develder, "Distributed multi-agent algorithm for residential energy management in smart grids," in *Proc. IEEE Network Operations and Management Symp. 2012 (NOMS 2012)*, Maui, HI, pp. 435–443.

[19] C. Patsios, B. Wu, E. Chatzinikolaou, D. J. Rogers, N. Wade, N. P. Brandon, and P. Taylor, "An integrated approach for the analysis and control of grid connected energy storage systems," *J. Energy Storage*, vol. 5, pp. 48–61, June 2016.

[20] C. Bussar, P. Stöckera, Z. Cai, L. Moraes, Jr., D. Magnor, P. Wiernes, N. van Brachtc, A. Moser, and D. U. Sauer, "Large-scale integration of renewable energies and impact on storage demand in a European renewable power system of 2050—Sensitivity study," *J. Energy Storage*, vol. 6, pp. 1–10, May 2016.

[21] M. Bila, C. Opathella, and B. Venkatesh, "Grid connected performance of a household lithium-ion battery energy storage system," *J. Energy Storage*, vol. 6, pp. 178–185, May 2016.

[22] X. Liu, P. Wang, and P. C. Loh, "A hybrid AC/DC microgrid and its coordination control," *IEEE Trans. Smart Grid*, vol. 2, no. 2, pp. 278–286, 2011.

[23] E. Hossain, E. Kabalci, R. Bayindir, and R. Perez, "Microgrid testbeds around the world: State of art," *Energy Conversion Manage.*, vol. 86, pp. 132–153, Oct. 2014.

[24] R. Bayindir, E. Bekiroglu, E. Hossain, and E. Kabalci, "Microgrid facility at European Union," in *Proc. 2014 Int. Conf. Renewable Energy Research and Application (ICRERA)*, Milwaukee, WI, pp. 865–872.

[25] W. F. Pickard, A. Q. Shen, and N. J. Hansing, "Parking the power: Strategies and physical limitations for bulk energy storage in supply–demand matching on a grid whose input power is provided by intermittent sources," *Renew. Sust. Energy Rev*, vol. 13, pp. 1934–1945, Oct. 2009.

[26] B. Dunn, H. Kamath, and J. Tarascon, "Electrical energy storage for the grid: A battery of choices," *Science*, vol. 334, no. 6058, pp. 928–935, 2011.

[27] G. Spagnuolo, G. Petrone, P. Mattavelli, and M. Guarnieri, "Vanadium redox flow batteries: Potentials and challenges of an emerging storage technology," *IEEE Ind. Electron. Mag.*, vol. 10, no. 4, pp. 20–31, 2016.

[28] J. Kondoh, I. Ishii, H. Yamaguchi, A. Murata, K. Otani, K. Sakuta, N. Higuchi, S. Sekine, and M. Kamimoto, "Electrical energy storage systems for energy networks," *Energy Convers. Manage.*, vol. 41, no. 17, pp. 1863–1874, 2000.

[29] P. Alotto, M. Guarnieri, and F. Moro, "Redox flow batteries for the storage of renewable energy: A review," *Renew. Sustain. Energy Rev.*, vol. 29, pp. 325–335, Jan. 2014.

[30] B. P. Roberts and C. Sandberg, "The role of energy storage in development of smart grids," *Proc. IEEE*, vol. 99, no. 6, pp. 1139–1144, 2011.

[31] I. Staffell and M. Rustomji, "Maximising the value of electricity storage," *J. Energy Storage*, vol. 8, pp. 212–225, Nov. 2016.

[32] Z. G. Yang. (2017, Oct. 26). It's big and long-lived, and it won't catch fire: The vanadium redox-flow battery. *IEEE Spectr.* [Online]. Available: https://spectrum.ieee.org/green-tech/fuel-cells/its-big-and-longlived-and-it-wont-catch-fire-the-vanadium-redoxflow-battery

[33] A. Zucker and T. Hinchliffe, "Optimum sizing of PV-attached electricity storage according to power market signals—A case study for Germany and Italy," *Appl. Energy*, vol. 127, pp. 141–155, Aug. 2014.

[34] M. R. Aghamohammadi and H. Abdolahinia, "A new approach for optimal sizing of battery energy storage system for primary frequency control of islanded microgrid," *Elect. Power Energy Syst.*, vol. 54, pp. 325–333, Jan. 2014.

[35] J. P. Fossati, A. Galarza, A. Martín-Villate, and L. Fontan, "A method for optimal sizing energy storage systems for microgrids," *Renew. Energy*, vol. 77, pp. 539–549, May 2015.

[36] S. X. Chen, H. B. Gooi, and M. Q. Wang, "Sizing of energy storage for microgrids," *IEEE Trans. Smart Grid*, vol. 3, no. 1, pp. 142–151, 2012.

[37] C. Goebel, H. Hesse, M. Schimpe, A. Jossen, and H.-A. Jacobsen, "Model-based dispatch strategies for lithium-ion battery energy storage applied to pay-as-bid markets for secondary reserve," *IEEE Trans. Power Syst.*, vol. 32, no. 4, pp. 2724–2734, 2017.

[38] Z. Ye, A. Kolwalkar, Y. Zhang, P. Du, and R. Walling, "Evaluation of anti-islanding schemes based on nondetection zone concept," *IEEE Trans. Power Electron.*, vol. 19, no. 5, pp. 1171–1176, 2004.

[39] V. John, Z. Ye, and A. Kolwalkar, "Investigation of anti-islanding protection of power converter based distributed generators using frequency domain analysis," *IEEE Trans. Power Electron.*, vol. 19, no. 5, pp. 1177–1183, 2004.

[40] S. P. Chowdhury, S. Chowdhury, and P. A. Crossley, "Islanding protection of active distribution networks with renewable distributed generators: A comprehensive survey," *Electric Power Syst. Res.*, vol. 79, no. 6, pp. 984–992, 2009.

[41] *Requirements for the Connection of Generators Above 16 A per Phase—Part 2: Connection to the MV Distribution System*, CENELEC Standard TS 50549-2, 2015.

[42] Y. Yang, F. Blaabjerg, and H. Wang, "Low-voltage ride-through of single-phase transformerless photovoltaic inverters," *IEEE Trans. Ind. Appl.*, vol. 50, no. 3, pp. 1942–1952, 2014.

[43] F. Katiraei, M. R. Iravani, and P. W. Lehn, "Micro-grid autonomous operation during and subsequent to islanding process," *IEEE Trans. Power Del.*, vol. 20, no. 1, pp. 248–257, 2005.

[44] F. Blaabjerg, R. Teodorescu, M. Liserre, and A. V. Timbus, "Overview of control and grid synchronization for distributed power generation systems," *IEEE Trans. Ind. Electron.*, vol. 53, no. 5, pp. 1398–1409, 2006.

[45] D. E. Olivares, A. Mehrizi-Sani, A. H. Etemadi, C. A. Cañizares, R. Iravani, M. Kazerani, M. Hajimiragha, O. Gomis-Bellmunt, M. Saeedifard, R. Palma-Behnke, G. A. Jiménez-Estévez, and N. D. Hatziargyriou, "Trends in microgrid control," *IEEE Trans. Smart Grid*, vol. 5, no. 4, pp. 1905–1919, 2014.

[46] A. Bidram and A. Davoudi, "Hierarchical structure of microgrids control system," *IEEE Trans. Smart Grid*, vol. 3, no. 4, pp. 1963–1976, 2012.

[47] E. Dall'Anese, H. Zhu, and G. B. Giannakis, "Distributed optimal power flow for smart microgrids," *IEEE Trans. Smart Grid*, vol. 4, no. 3, pp. 1464–1475, 2013.

[48] M. T. Lawder, B. Suthar, P. W. C. Northrop, A. De, C. M. Hoff, O. Leitermann, M. L. Crow, S. Santhanagopalan, and V. R. Subramanian, "Battery energy storage system (BESS) and battery management system (BMS) for grid-scale applications," *Proc. IEEE*, vol. 102, no. 6, pp. 1014–1030, 2014.

[49] J. M. Guerrero, J. C. Vasquez, J. Matas, L. G. de Vicuña, and M. Castilla, "Hierarchical control of droop-controlled ac and dc microgrids—A general approach toward standardization," *IEEE Trans. Ind. Electron.*, vol. 58, no. 1, pp. 158–172, 2011.

[50] F. Katiraei and M. R. Iravani, "Power management strategies for a microgrid with multiple distributed generation units," *IEEE Trans. Power Syst*, vol. 21, no. 4, pp. 1821–1831, 2006.